Synthesis of epitaxial Sn_xGe_{1-x} alloy films by ion-assisted molecular beam epitaxy

Gang He[a] and Harry A. Atwater
Thomas J. Watson Laboratory of Applied Physics, California Institute of Technology, Pasadena, California 91125

(Received 12 July 1995; accepted for publication 21 November 1995)

In this letter, we report the synthesis of epitaxial Sn_xGe_{1-x}/Ge/Si(001) with compositions up to $x=0.34$ by ion-assisted molecular beam epitaxy with 30–100 eV Ar^+ ions produced by an electron cyclotron resonance ionization source with ion to atom flux ratios of the order of unity in the substrate temperature range of 120–200 °C. High flux low energy ion beam irradiation greatly inhibits Sn segregation without interrupting epitaxy. © *1996 American Institute of Physics.* [S0003-6951(96)02805-6]

The metastable Sn_xGe_{1-x} alloy system is an interesting group IV semiconductor material with potential applications in the fabrication of Si-based high performance heterojunction devices and long wavelength infrared optoelectronic devices. Band structure calculations have suggested that, while Sn is a semimetal and Ge is an indirect band gap semiconductor, diamond cubic Sn_xGe_{1-x} alloys may have direct band gaps continuously tunable from 0.55 to 0 eV for compositions x from 0.2 to 0.6, with very low electron masses and hence high electron mobilities.[1–4]

Many growth techniques, including molecular beam epitaxy,[5–12] sputter deposition,[13] and solid phase recrystallization,[14–16] have been used to synthesize both epitaxial and polycrystalline Sn_xGe_{1-x} thin films. Although bulk Sn transforms from α phase (diamond cubic) to β phase (body-centered tetragonal) at 13.2 °C,[17] thin film α-Sn can be epitaxially stabilized on substrates with similar lattice constants at much higher temperatures (~130 °C).[18–21] However, Sn_xGe_{1-x} alloys with compositions that lead to confirmed direct band gaps have not been achieved to date. Synthesis of Sn_xGe_{1-x} alloys in the direct gap composition range has proved to be difficult due to the severe surface Sn segregation during conventional thermal growth.[12] Sn_xGe_{1-x} is a simple eutectic system (eutectic temperature ~231 °C)[22,23] with mutual equilibrium solubilities no more than 1 at.%,[24,25] much less than the compositions required for a direct band gap. Driven by the surface free energy difference and the limited solid solubility between Sn and Ge, Sn tends to segregate to the surface during growth.[5–13] The difference in atomic radii between Sn and Ge (about 13%) may also play a role in the surface Sn segregation when Sn_xGe_{1-x} is deposited on a lattice mismatched substrate that generates a coherency strain field. Both the present results and results of previous investigations[12] suggest that in order to obtain Sn_xGe_{1-x} with compositions in the direct band gap range by conventional thermal epitaxial growth, the surface segregation of Sn must be suppressed by reducing the growth temperature to a level at which surface kinetic roughening is significant enough to cause a breakdown of epitaxy. Similar breakdown of epitaxy caused by surface kinetic roughening has been studied in low temperature silicon homoepitaxy.[26,27]

To overcome the conflicting requirements posed by the Sn surface segregation and the surface kinetic roughening during conventional thermal growth, we investigated the growth of epitaxial Sn_xGe_{1-x}/Ge/Si(001) by ion-assisted molecular beam epitaxy. When the growing surface of a thin film is bombarded by low energy ions, the surface atoms undergo subsurface recoil implantation and generate collisional mixing between the surface and subsurface layers without producing extended bulk crystal damage,[28] and hence incorporate surface atoms into the growing epitaxial film. We used an electron cyclotron resonance (ECR) ion source with high purity Ar gas to generate low energy high flux ion beams at relatively low pressures (0.1–1 mTorr). Ion energies in the range of 30–100 eV produce near-surface collisional mixing while avoiding ion damage to the bulk crystal, enabling synthesis of single-crystal epitaxial Sn_xGe_{1-x} with Sn compositions up to $x=0.34$, which are within the predicted direct band gap composition range.

The epitaxial Sn_xGe_{1-x} alloys were grown in a custom-designed molecular beam epitaxy system with a base pressure of about 3×10^{-10} Torr. The system is pumped by a cryopump and equipped with reflection high energy electron diffraction (RHEED) (14 keV electron beam) for *in situ* surface analysis. High purity (99.9999%) Ge and Sn solid sources were used for deposition by electron beam evaporation and Knudsen effusion, respectively. The film thickness and deposition rate are controlled by quartz crystal thickness monitors. The total growth rate is set at around 0.05 nm/sec. The ion source is a 250 W ECR source with excitation at 2.45 GHz and uses high purity Ar gas (99.9995%) at a typical background pressure of 0.15 mTorr with a 10 sccm flow rate. The substrate can be electrically biased relative to ground, and is about 20 cm away from the ECR ion source. Calibrations indicate that the ion energy was in the range of 30–50 eV when the substrate is grounded, and the ion current at the substrate is about 0.04 mA/cm^2, which corresponds to an ion-to-atom flux ratio of the order of unity. Most samples were deposited with the substrate grounded. All the substrates were Si(001) wafers and were chemically cleaned (in H_2O:H_2O_2:NH_4HNO_4 5:1:1 for 10 min) and hy-

[a]Electronic mail: ghe@daedalus.caltech.edu

 0003-6951/96/68(5)/664/3/$10.00

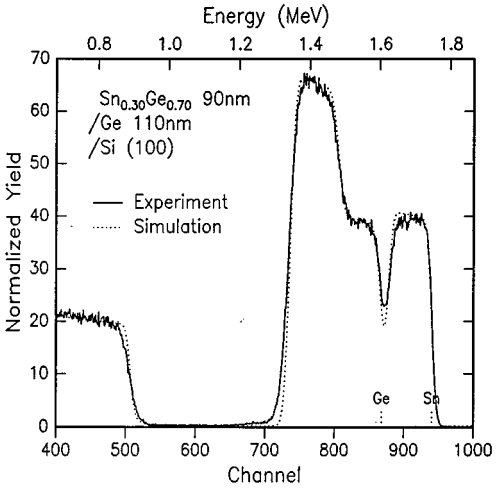

FIG. 1. 2 MeV H^{++} Rutherford backscattering spectrum of 90 nm $Sn_{0.30}Ge_{0.70}$/Ge/Si(001) grown with ion irradiation at 200 °C. The solid curve is the experimental data and the dashed curve is a simulation of the same film structure by RUMP. The spectrum confirms the alloy composition and indicates a uniform composition profile.

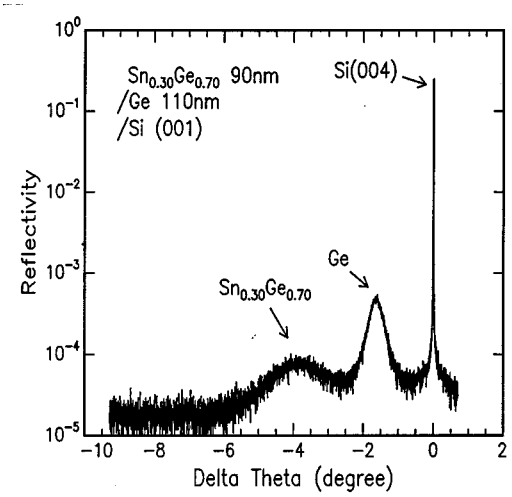

FIG. 2. High resolution x-ray diffraction of a 90 nm $Sn_{0.30}Ge_{0.70}$/Ge/Si(001) grown with ion irradiation at 200 °C. The (004) diffraction peak shifts are consistent with homogeneous diamond cubic $Sn_{0.30}Ge_{0.70}$ within the virtual crystal approximation. The Ge and Sn_xGe_{1-x} peak widths may be attributed to the small film thickness and the misfit dislocations in the films resulted from the expected strain relaxation caused by the substrate lattice mismatch, as well as the possible compositional nonuniformity of the alloy film in the case of Sn_xGe_{1-x}.

drogen terminated (by dipping in 10% HF/H_2O) prior to transfer into the ultrahigh vacuum deposition chamber. Following *in situ* prebakes at 200 °C for 2 h, the substrates were heated to 550 °C to desorb the surface hydrogen and produce a (2×1) reconstructed Si(001) surface. Epitaxial Ge buffer layers of 100 to 200 nm were then deposited at 400 °C. The finished Ge buffer layer surfaces were also (2×1) reconstructed and smooth (as judged qualitatively with RHEED observations). The substrates were then cooled to temperatures ranging from 120 to 200 °C and Sn_xGe_{1-x} layers were deposited in the composition range of $x=0.1-0.4$ with or without ion irradiation. *In situ* RHEED patterns along the [110] direction were recorded throughout growth by video data acquisition. Samples were characterized following growth by optical microscopy, Rutherford backscattering spectroscopy with 2 MeV He^{++}, high resolution x-ray diffraction with Cu $K\alpha_1$ x rays, and transmission electron microscopy (TEM).

None of the thermally grown Sn_xGe_{1-x} samples achieved Sn compositions larger than $x=0.2$. At 120 °C growth temperature, *in situ* RHEED analysis showed that for samples with $x<0.2$ the Sn_xGe_{1-x} films remained epitaxial with atomically rough surfaces for a finite thickness (a few tens of nanometers) and then gradually transformed to amorphous films, and for samples with $x>0.2$, the surface RHEED evolved rapidly to a more diffusive amorphous pattern of lower diffraction contrast within a few nanometers of Sn_xGe_{1-x} growth. We speculate that the lower diffraction contrast may be caused by a strongly segregated Sn layer that covered the film surface. All samples grown at 120 °C had optically smooth surfaces. At 200 °C, samples were grown with compositions in the range $x=0.2-0.3$. *In situ* RHEED analysis showed that for these compositions, the Sn_xGe_{1-x} film surfaces became atomically rough and the diffraction intensity slowly decreased, but never completely disappeared, as the film thickness increased to over 100 nm. Optical microscopy revealed surfaces of these samples that were optically rough with ~1 μm sized droplets. Rutherford backscattering analysis showed strong surface Sn segregation. The combination of these analyses also suggested that during the 200 °C thermal growth, the Sn and Ge phases separated and the film surfaces were partially occupied by epitaxial Ge-rich regions of decreasing size, which is consistent with the observed decreasing RHEED intensity as a function of time. At either growth temperature, epitaxial Sn_xGe_{1-x} films with $x>0.2$ could not be achieved. These results were consistent with the suggestion that the breakdown of epitaxy was caused by the constraints of either surface kinetic roughening at low temperatures or surface Sn segregation at high temperatures, which cannot be easily overcome by thermal growth.[12]

Samples grown with ion irradiation showed different results. For samples grown in the range of 140–160 °C with ion-to-atom flux ratio of about unity, *in situ* RHEED during Sn_xGe_{1-x} growth showed a gradual transition from surface roughening (at 10 nm film thickness) to twinning (at 20 nm film thickness) and eventually to polycrystalline transformation (at 50–100 nm film thickness) for compositions $x<0.35$, and slowly decreasing diffraction intensity that eventually led to an amorphous pattern with low diffraction contrast for compositions $x>0.35$. Optical inspection showed that the sample surfaces were optically smooth for $x<0.35$ and optically rough with ~1 μm sized droplets for $x<0.35$. Backscattering spectra confirmed the Sn_xGe_{1-x} film compositions and showed that for the optically smooth samples ($x<0.35$), Sn was completely incorporated into the Sn_xGe_{1-x} films, while for the optically rough samples ($x>0.35$), Sn segregated to the surface. Single crystal epitaxial $Sn_{0.34}Ge_{0.66}$ samples up to 20 nm thick and polycrystalline $Sn_{0.30}Ge_{0.70}$ samples more than 200 nm thick were obtained

by ion-assisted growth at 150 °C with uniform composition profiles confirmed by RBS. Note that these compositions are within the range of the predicted direct band gap.

Ion-assisted growth was also carried out at 200 °C, and a different growth mode was observed at this temperature. For a series of samples with compositions in the range of $x = 0.2-0.3$, RHEED indicated atomically rough surfaces, but a single crystal diffraction pattern persisted with no evidence of twinning throughout the growth. For compositions $x > 0.3$, the RHEED intensity started to decrease after about 90 nm of Sn_xGe_{1-x} film growth. Optical microscopy inspections revealed that the sample surfaces were optically smooth except for thick (>100 nm) Sn_xGe_{1-x} samples with $x > 0.3$. Backscattering spectra showed that Sn incorporated completely into the Sn_xGe_{1-x} alloy films for the optically smooth samples. For a few samples, in which ion energy was increased to about 100 eV by substrate biasing, backscattering spectra showed Ar inclusions of approximately 1 at.% in the epitaxial Sn_xGe_{1-x} films. No Ar inclusions were detectable by backscattering for samples grown with grounded substrates (i.e., ion energies of about 40 eV). Epitaxial $Sn_{0.30}Ge_{0.70}$ films up to 90 nm and $Sn_{0.26}Ge_{0.74}$ films up to 230 nm were obtained by ion-assisted growth at 200 °C. Backscattering spectra confirmed uniform composition profiles, as shown in Fig. 1. High resolution x-ray diffraction of the (004) diffraction peak from the Sn_xGe_{1-x} films produced peak shifts consistent with diamond cubic Sn_xGe_{1-x} with lattice constants consistent with the virtual crystal approximations as illustrated in Fig. 2. The relatively wide width of the x-ray diffraction peak from the Sn_xGe_{1-x} film may be attributed to the small Sn_xGe_{1-x} film thickness and the misfit dislocations in the film resulted from the expected strain relaxation caused by the substrate lattice mismatch, as well as the possible small compositional nonuniformity of the alloy film. Cross-sectional transmissional electron microscopy analysis also confirmed epitaxial Sn_xGe_{1-x} films with sharp interfaces, and the selected area electron diffraction patterns from the Sn_xGe_{1-x} films and the Ge buffer layers are consistent with their lattice parameter differences within the virtual crystal approximation.

In summary, thermal growth of epitaxial Sn_xGe_{1-x} faces great difficulty in achieving the compositions required for direct band gap Sn_xGe_{1-x} alloys due to a breakdown of epitaxy caused by ether surface Sn segregation at high temperatures or surface kinetic roughening at low temperatures. Irradiation of the film surface with a low energy (30–100 eV) high flux (ion/atom ~ 1) ion beam can efficiently suppress Sn surface segregation. Compositionally homogeneous epitaxial diamond cubic Sn_xGe_{1-x} alloy films with Sn compositions as high as 0.30–0.34 have been achieved with ion-assisted MBE using ECR Ar^+ ion source. We note that epitaxial Sn_xGe_{1-x} films with even higher compositions may be possible by optimizing the ion-assisted MBE growth parameters, including growth temperature, growth rate, ion energy, ion flux, ion species, as well as substrate type. Achievement of a higher ion flux seems likely to be the most straightforward approach to further increase the incorporation of Sn during growth. Use of heavier ion species (e.g., Xe) may also improve the Sn incorporation by better matched energy transfer to the Sn surface atoms. We note also that if ion-assisted growth is combined with nearly lattice-matched substrates, e.g., InP,[6] high quality dislocation free single crystal Sn_xGe_{1-x} films in the direct band gap region may be possible.

This work was supported by the National Science Foundation under Grant No. DMR-9503210. We also acknowledge the expert technical assistance of M. Easterbrook and C. M. Garland.

[1] D. W. Jenkins and J. D. Dow, Phys. Rev. B **36**, 7994 (1987).
[2] B. I. Craig, Superlattices Microstruct. **12**, 1 (1992).
[3] H. A. Atwater, G. He, and C. Saipetch, Mater. Res. Soc. Symp. Proc. (to be published).
[4] E. Kaxiras (unpublished).
[5] A. Harwit, P. R. Pukite, J. Angilello, and S. S. Iyer, Thin Solid Films **184**, 395 (1990).
[6] J. Piao, R. Beresford, T. Licata, W. I. Wang, and H. Homma, J. Vac. Sci. Technol. B **8**, 221 (1990).
[7] W. Wegscheider, K. Eberl, U. Menczigar, and G. Abstreiter, Appl. Phys. Lett. **57**, 875 (1990).
[8] H.-J. Gossmann, J. Appl. Phys. **68**, 2791 (1990).
[9] E. A. Fitzgerald, P. E. Freeland, M. T. Asom, W. P. Lowe, R. A. Macharrie, Jr., B. E. Weir, A. R. Kortan, F. A. Thiel, Y.-H. Xie, A. M. Sergent, S. L. Cooper, G. A. Thomas, and L. C. Kimerling, J. Electron. Mater. **20**, 489 (1991).
[10] K. Eberl, W. Wegscheider, and G. Abstreiter, J. Cryst. Growth **111**, 882 (1991).
[11] P. Vogl, J. Olajos, W. Wegscheider, and G. Abstreiter, Surf. Sci. **267**, 83 (1992).
[12] W. Wegscheider, J. Olajos, U. Menczigar, W. Dondl, and G. Abstreiter, J. Cryst. Growth **123**, 75 (1992).
[13] S. I. Shah, J. E. Greene, L. L. Abels, Q. Yao, and P. M. Raccah, J. Cryst. Growth **83**, 3 (1987).
[14] S. Oguz, W. Paul, T. T. Deutsch, B.-Y. Tsaur, and D. V. Murphy, Appl. Phys. Lett. **43**, 848 (1983).
[15] I. T. H. Chang, B. Cantor, and A. G. Cullis, J. Non-Cryst. Solids **117/118**, 263 (1990).
[16] S. M. Lee, J. Appl. Phys. **75**, 1987 (1994).
[17] W. Klemm and H. Stöhr, Z. Anorg. Allg. Chem. **241**, 305 (1939).
[18] R. F. C. Farrow, D. S. Robertson, G. M. Williams, A. G. Cullis, G. R. Jones, I. M. Young, and P. N. J. Dennis, J. Cryst. Growth **54**, 507 (1981).
[19] J. L. Reno and L. L. Stephenson, Appl. Phys. Lett. **54**, 2207 (1989).
[20] M. T. Asom, A. R. Kortan, L. C. Kimerling, and R. C. Farrow, Appl. Phys. Lett. **55**, 1439 (1989).
[21] T. Ito, Jpn. J. Appl. Phys. **31**, L920 (1992).
[22] T. Soma, H. Matsuo, and S. Kagaya, Phys. Status Solidi **105**, 311 (1981).
[23] T. B. Massalski, *Binary Alloy Phase Diagrams* (American Society of Metals, Metals Park, OH, 1986), Vol. 2.
[24] C. D. Thurmond, J. Phys. Chem. **57**, 827 (1953).
[25] C. D. Thurmond, F. A. Trumbore, and M. Kowalchik, J. Chem. Phys. **24**, 799 (1956).
[26] D. J. Eaglesham, H.-J. Gossman, and M. Cerullo, Phys. Rev. Lett. **65**, 1227 (1990).
[27] M. V. R. Murty and H. A. Atwater, Phys. Rev. B **49**, 8483 (1994).
[28] M. V. R. Murty and H. A. Atwater, Phys. Rev. B **45**, 1507 (1992).
[29] G. He and H. A. Atwater, Nucl. Instrum. Methods B (to be published).